Journal of Materials Chemistry B

PAPER

View Article Online
View Journal

Cite this: DOI: 10.1039/c9tb00168a

Understanding how charge and hydrophobicity influence globular protein adsorption to alkanethiol and material surfaces†

Simon J. Attwood, *[a] Rebecca Kershaw,[a] Shahid Uddin,[b] Steven M. Bishop[c] and Mark E. Welland[a]

Received 24th January 2019,
Accepted 28th February 2019

DOI: 10.1039/c9tb00168a

rsc.li/materials-b

Every biosensor, bioengineered scaffold or biomedical implant depends crucially on an ability to control protein adsorption at the material surface. Yet the adsorption of proteins to solid surfaces in aqueous media is a complex and poorly understood phenomenon. To gain further insights we study protein adsorption using the quartz crystal microbalance for 10 model globular proteins interacting with positive, negative, neutral, hydrophobic and mixed alkanethiol monolayers as well as silica, polystyrene and Teflon, equating to approximately 200 protein–surface combinations. The charge state of the materials in liquid was measured with atomic force microscopy using a colloidal probe and numerically solving the full non-linear Poisson–Boltzmann equation. This approach has allowed us to address some of the important questions surrounding the basic principles that govern protein adsorption including the relative importance of net charge and hydrophobicity and why some materials are protein resistant. With our set of mixed monolayer surfaces, we can modulate charge over a wide range whilst eliminating hydrophobic interactions and *vice versa* – thus permitting determination of the functional dependence of adsorption on these parameters. This has led us to develop two empirical predictive models with up to 90% accuracy that together encompass most materials relevant to biotechnological and biomedical applications.

Introduction

The first event that initiates the biological response to artificial materials is the adsorption of proteins.[1–3] To effectively design materials for advanced biomedical devices a fundamental understanding of what governs protein adsorption must be established. Protein adsorption has been studied extensively for over five decades leading to a substantive body of literature on the topic.[2,4–12] In a recent review article Vogler[9] commented that *"Anyone closely examining this literature in its entirety will be struck by a lack of consensus so extreme that nearly no general conclusions can be extracted."* Similar comments have been made by other authors;[8] *"...a unified predictive theory is still missing, even though the adsorption of proteins from aqueous solution onto solid surfaces has been studied extensively for 40 years."* Rabe[7] commented that Nakanishi's[13] assessment a decade earlier of protein adsorption as *"...a common but very complicated phenomena"* was still very much valid. Answers to specific and basic questions such as "do proteins adsorb more to hydrophobic or hydrophilic surfaces?" or "is charge more important than hydrophobicity?"[2,7] lack general agreement and remain controversial. Due to the energetic cost of displacing water it has been suggested that proteins should not adsorb to hydrophilic surfaces, and there is experimental evidence to back up this theory[9,14] yet there is also strong evidence that proteins do adsorb to hydrophilic surfaces.[10] There is also a lack of understanding as to why coatings such as polyethylene glycol or zwitterionic polymers[15] have such good anti-fouling properties.[7] There are numerous models in the literature that help explain the dynamics and kinetics of protein adsorption. What is currently lacking is a robust empirical model that links the physical properties of a material to the extent of protein adsorption, which would aid the rational design of biomaterials.

Part of the problem is that measurement of adsorption is highly dependent on the analytical technique, but even when the same techniques are used results are typically inconsistent due to there being no standardized set of procedures. Furthermore, typically only one or two proteins are considered in any given study which makes drawing broad conclusions difficult. To resolve this problem and help reconcile some of the

[a] Nanoscience Centre, University of Cambridge, J. J. Thomson Avenue, CB3 0FF, UK. E-mail: simonjamesattwood@gmail.com
[b] Department of Dosage Form Design and Development, MedImmune Ltd., Aaron Klug Building, Granta Park, Cambridge CB21 6GH, UK
[c] Department of Dosage Form Design and Development, MedImmune, One MedImmune Way, Gaithersburg, Maryland 20878, USA

† Electronic supplementary information (ESI) available. See DOI: 10.1039/c9tb00168a

controversies in the literature we employed a survey-style approach – that is we study many protein–surface combinations under carefully controlled, homogenous experimental conditions.

For detection we utilize a quartz crystal microbalance (QCM) setup which employs acoustic, time-resolved mass sensing with very high sensitivity.[16] A drawback to the QCM is that in addition to sensing the 'dry mass' of the protein it also has a contribution from hydrodynamically coupled water meaning the overall 'wet mass' measurement is somewhat higher than the true protein mass. Whilst the contribution from water varies depending on protein size and shape, for similar sized globular proteins, such as we study here, the relative differences are negligible.[17] Dissipation for these proteins is also low meaning the Sauerbrey equation is a valid approach for calibrating frequency shifts. There are also several advantages to using the QCM over other techniques. Since we are measuring wet mass, at low coverages there is a large signal amplification effect meaning the lower limit of detection is far below that of other optical techniques – thus allowing us to effectively measure and compare weakly adsorbing proteins. Whilst most other techniques such as surface plasmon resonance (SPR) or dual polarization interferometry (DPI) are limited to very specific types of sensor surface, the QCM is unrivalled in that almost any surface is amenable to detection with the QCM including metals, metal oxides, glass, polymers and alkanethiols on gold.

We have also taken great care to prepare surfaces with well-defined chemistries. Primarily we use alkanethiol monolayers on gold[18,19] which form semi-crystalline surfaces and permit us to tailor the chemistry. We used an advanced atomic force microscopy approach to determine the surface potential of all our surfaces in liquid. Measuring the charge state of flat materials in liquid is very difficult by any other technique. Protein adsorption to alkanethiol monolayers has been studied before with other techniques but with only a few protein–surface combinations.[18–25]

By applying this survey-style approach in conjunction with carefully prepared and characterized surfaces and assessing protein adsorption under homogeneous experimental conditions we have been able to address many of the outstanding questions regarding the basic principles of protein adsorption. Having seen that charge and hydrophobicity are the primary drivers of adsorption we set out to see if a simple measure of material surface charge and hydrophobicity is enough to permit a prediction of protein adsorption extent. We are primarily interested in developing an empirical model that predicts protein adsorption and are less interested in whether the model is based on a rigorous physical representation of protein dynamics at the molecular level. Such a prediction may guide bioengineers when choosing surfaces for biomedical applications. There are many reasons why the classical Langmuir law is not valid[26] to describe protein adsorption but we show that the most significant factor is the violation of the requirement for proteins to be non-interacting. By empirically accounting for this we develop a model that shows up to 90% prediction accuracy for charged surfaces, therefore justifying our approach. Adsorption on surfaces that have both charge and hydrophobic contributions are very complicated to predict and so for the current work we restrict ourselves to the study of either 'charged' or 'hydrophobic' surfaces. We define the former as having a contact angle $\sim 10^\circ$ and the latter as any contact angle 0–125°, with some obvious degree of overlap. We use mixed alkanethiol monolayers that allow us to either largely exclude hydrophobic interactions whilst controlling charge or largely exclude charge interactions whilst controlling hydrophobicity. This allows us to determine the functional dependence of adsorption on either charge or hydrophobicity.

Results

Surface characterization

To assess the charge state of our surfaces in aqueous media we use the atomic force microscopy (AFM) approach pioneered by Ducker *et al.*[27] The potential of a silica colloid attached to an AFM cantilever and a flat silica substrate was first measured. The force–displacement profile is clearly repulsive (Fig. 1b) at pH = 7 with a measured potential of -23 ± 1 mV. As shown in Fig. 1c the potential falls towards zero around pH = 2, which agrees with the known point of zero charge for silica.[28] With the tip potential determined we could then probe the potential of different surfaces. Alkanethiol monolayers were prepared from ethanolic solutions of SH-$(CH_2)_{10}$–R. We chose two negative surfaces (R = COOH, R = H_2PO_3), two positive surfaces (R = $N(CH_3)_3$, R = EG_6NH_2), a neutral hydrophilic (R = OH) and a neutral hydrophobic (R = CH_3) surface which we confirm with AFM measurements (Fig. 1d and e). We also characterized the surfaces by static contact angle measurements (Fig. 1f–i). The contact angles for COOH ($3.5 \pm 0.4^\circ$), OH ($11 \pm 2^\circ$) and CH_3 ($111 \pm 4^\circ$) surfaces are in good agreement with previous studies,[29] indicating our protocol was sufficient to produce good quality monolayers. For mixed monolayers we define χ_c = [COOH]/([COOH] + [OH]) and χ_h = $[CH_3]/([CH_3] + [OH])$. For mixed CH_3/OH surfaces we find the measured contact angles increase with χ_h and span the range from 11–111°. These surfaces thus allow us to tailor the hydrophobicity whilst keeping the charge neutral. In contrast the COOH/OH surfaces allow us to vary the surface potential from neutral to −21 mV whilst minimizing hydrophobic effects.

Charge and hydrophobicity govern adsorption

We measured the adsorption of the 10 proteins (Fig. S1, ESI†) to each of the 6 pure alkanethiol surfaces (Fig. 2) using the QCM. Since the surface bound nanoscale globular proteins represent a laterally heterogenous film the Sauerbrey equation is only valid[30] if $\Delta D/(\Delta f/n) \ll 4 \times 10^{-7}$. As shown in ESI† Table S2 this is true for all the proteins presented here. We sample the coverage at t = 400 s, where typically coverage has plateaued or significantly slowed (ESI,† Fig. S2) and compare this to the value pH–pI. As discussed later the application of more advanced kinetic models is controversial and so we opt for this basic strategy as a starting point. If the value of pH–pI is negative the protein possesses a net positive charge and if the

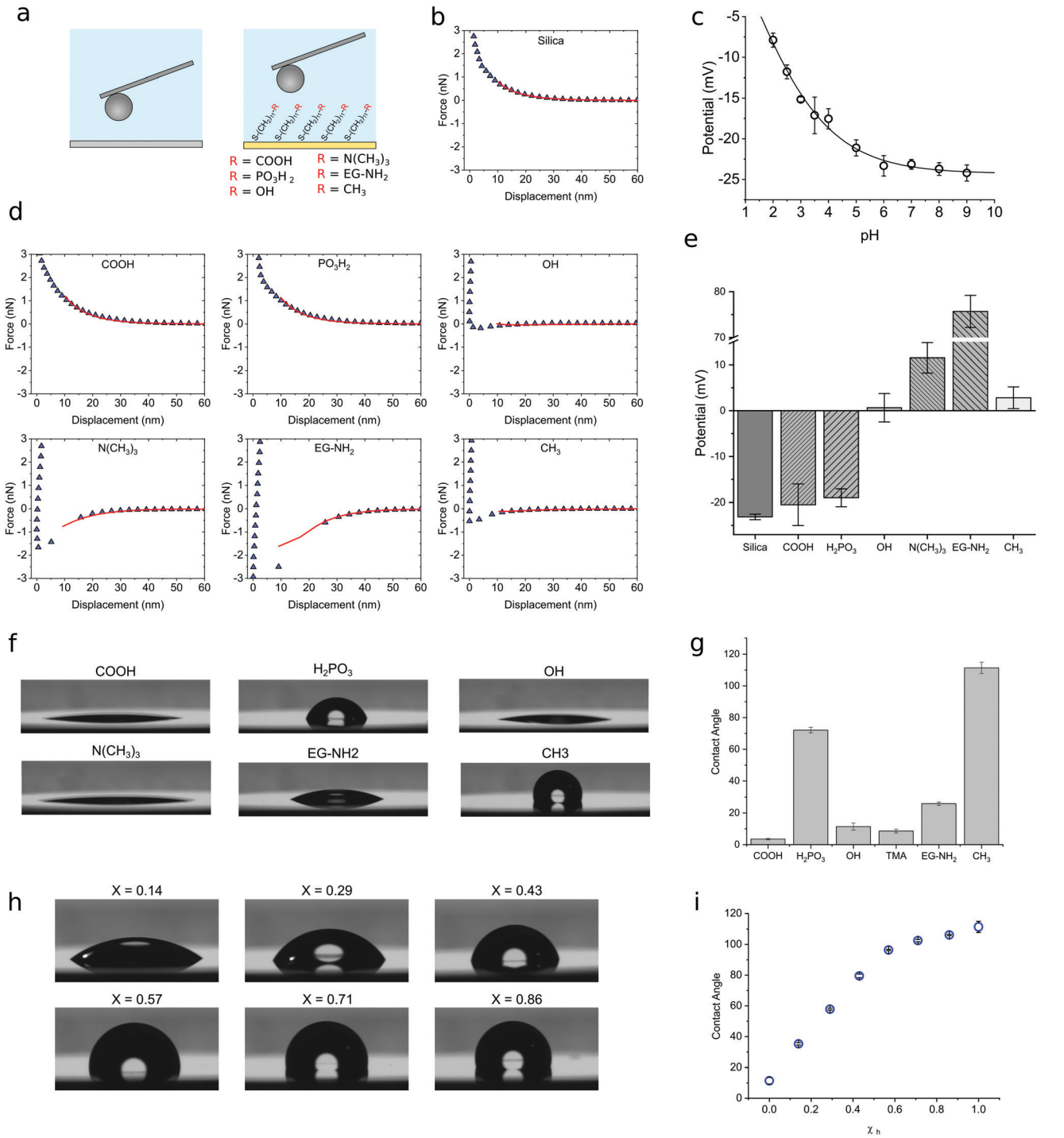

Fig. 1 Characterization of materials by atomic force microscopy to determine surface potential in liquid and contact angle measurements. (a) Schematics illustrating an AFM cantilever modified with a silica microsphere interacting in liquid with a Silica substrate (left) and model alkanethiol monolayers (right). Six pure alkanethiol surfaces were prepared with general formula SH-$(CH_2)_{10}$–R including two negatively charged (R = COOH, H_2PO_3), two positively charged (R = $N(CH_3)_3$, NH_2) and two charge-neutral (R = OH, CH_3). (b) Tip force as a function of separation for a silica tip on a silica surface at pH = 7. Blue triangles represent averages of 100 individual force–displacement plots. Solid red line is a fit to DLVO theory where the electrostatic contribution is found from a numerical solution to the full non-linear Poisson–Boltzmann equation (Ducker1991) with the constant charge boundary condition. (c) The potential of a silica surface was determined for a range of buffers (pH = 2–9) by fitting the DLVO theory to force–displacement curves. Values are averages of repeats from separate experiments. (d) Force–displacement curves for a silica tip interacting with the six alkanethiol monolayer surfaces (blue triangles) together with fits to DLVO theory (solid red line). (e) Potentials determined for all six alkanethiol surfaces plus silica with averages determined from repeats of separate experiments. (f) Water droplets (10 mM phosphate buffer, pH = 7) pictured on the six alkanethiol surfaces. (g) Measured contact angles. (h) Water droplets pictured on mixed OH/CH_3 surfaces with χ_h = [CH_3]/([CH_3] + [OH]) where [COOH], [OH] and [CH_3] represent respectively the bulk concentrations of carboxyl, hydroxyl, and methyl terminating alkanethiols. (i) Measured contact angles.

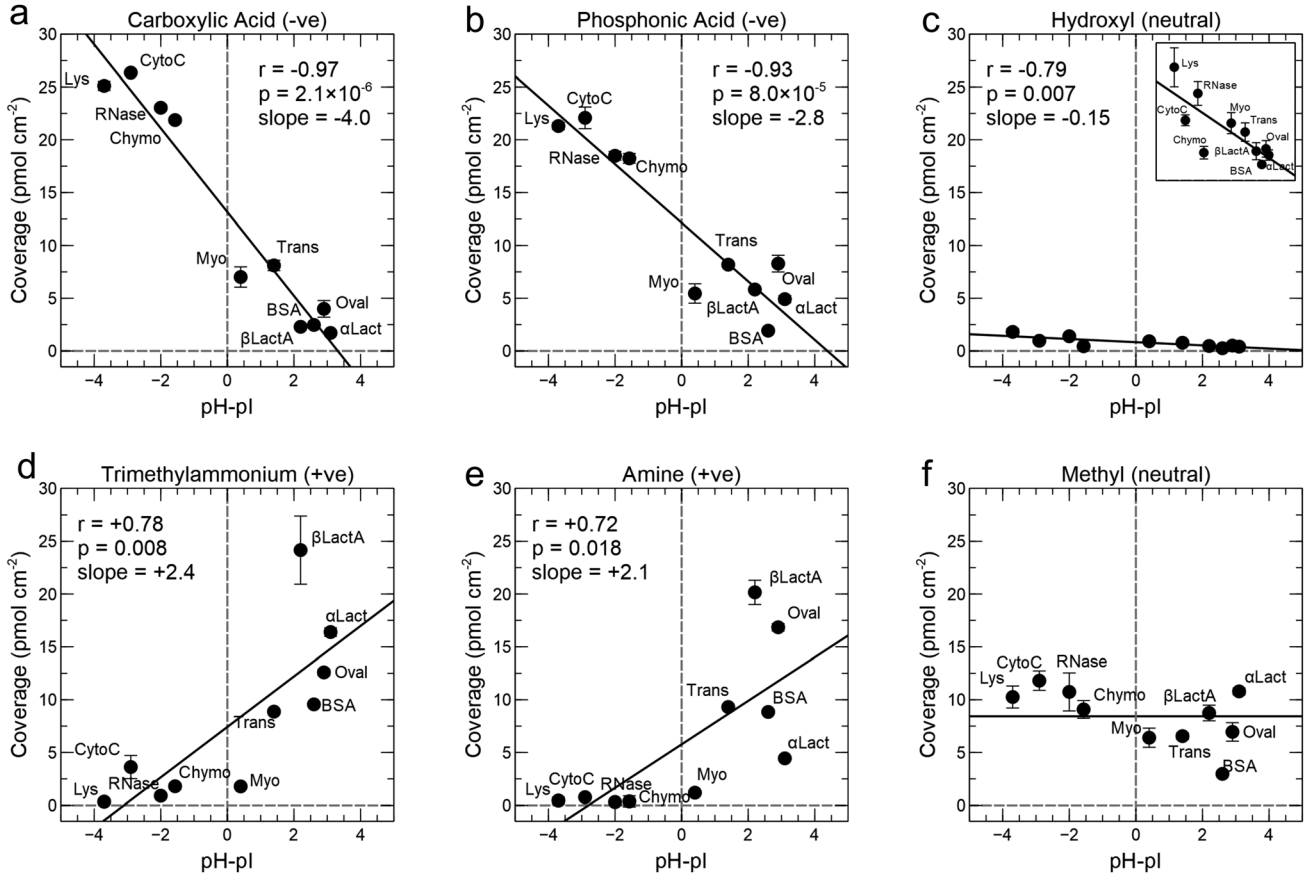

Fig. 2 Protein adsorption of ten globular proteins to six alkanethiol monolayer surfaces measured by quartz crystal microbalance. (a–f) Coverage (sampled at arbitrary t = 400 s) plotted against pH–pI (data points are averages of 3 repeat experiments, error bars SEOM). The proteins are lysozyme (Lys), cytochrome *C* (Cyto), ribonuclease A (RNase), chymotrypsinogen A (Chymo), myoglobin (Myo), apo-transferrin (apo-Trans), β-lactoglobulin (β-Lact), bovine serum albumin (BSA), ovalbumin (Oval), α-lactalbumin (α-Lact). All protein concentrations are 1 μM, buffer is 10 mM phosphate at pH = 7.4. See ESI† Fig. S2 for raw data.

value of pH–pI is positive the protein possesses a net negative charge. Clearly there are strong correlations, broadly demonstrating that when the surface and protein have opposite polarity adsorption is high, whereas when they possess the same polarity adsorption is minimal. We also used dual polarization interferometry (DPI)[31,32] which measures the 'dry mass' as opposed to the 'wet mass'. As expected, the absolute values are approximately 50% lower for the DPI measurements of the proteins on negatively charged siliconoxynitride, however the overall trend is very similar (ESI,† Fig. S5). This confirms that any differences in hydrodynamically coupled water between these small globular proteins is minimal and the QCM is a valid approach for comparing relative extent of adsorption in this case. For comparison we also show (ESI,† Fig. S5) that the trend is conserved on all negatively charged surfaces we measured: COOH, H_2PO_3, Silica and siliconoxynitride. Strikingly all proteins are in contrast strongly inhibited from adsorbing to the neutral hydrophilic hydroxyl surface. The 4 proteins that possess a net positive charge exhibit an average 95% reduction in coverage when on the OH surfaces as compared to on the negative COOH surface. Similarly, the 5 proteins that possess a strong net negative charge exhibit an average 96% reduction in coverage when on the OH surfaces as compared to the positive N–$(CH_3)_3$ surfaces. As a minor effect we do see a significant correlation with an order of magnitude reduced slope that might indicate the surface possesses a slight negative charge. If this is the case it is below the detection limit of the AFM measurements. On the neutral hydrophobic methyl surfaces all proteins adsorb at an intermediate level, with no significant correlation with protein charge. This illustrates that the two main driving forces for protein adsorption to solid surfaces are charge and hydrophobicity – when the hydrophobic force and charge interactions are minimized as is the case for the OH surface there is little tendency for the proteins to adsorb. The low adsorption of proteins to the OH surface agrees with previous work.[33] In that study they also demonstrate that monolayers comprised of R = EG_6–OH where EG = ethylene glycol (CH_2CH_2O) exhibit superior anti-fouling properties. This molecule is both charge neutral and hydrophilic but the long flexible ethylene glycol chains further resist protein adsorption through entropic effects.

Functional form of coverage dependence on charge and hydrophobicity

To understand protein adsorption in more detail it is initially necessary to focus on one protein, although we later confirm

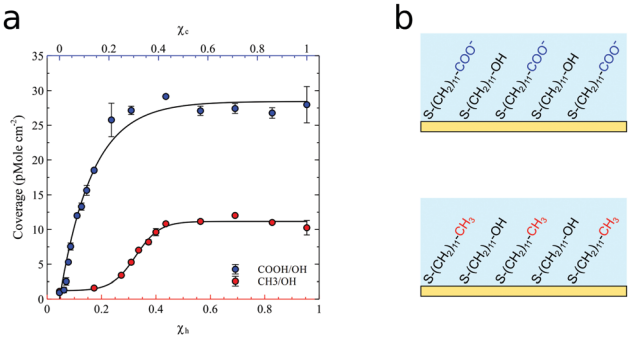

Fig. 3 Adsorption of proteins to mixed monolayers. (a) Adsorption coverage of lysozyme on 16 COOH/OH mixed monolayer surfaces in the range χ_c = 0–1 (blue circles, upper *x* axis). We fit the data to a saturable exponential of empirical form $m = a_1(1 - e^{-b_1\chi_c})$ where a_1 = 28.4 and b_1 = 7.6. Adsorption coverage of lysozyme on 12 CH_3/OH mixed monolayer surfaces in the range χ_h = 0–1 (red circles, lower *x* axis). We fitted the empirical equation $m = \frac{a_2 10^{b_2(\chi_h - c_2)}}{1 + 10^{b_2(\chi_h - c_2)}} + d_2$ with a_2 = 9.98, b_2 = 9.03, c_2 = 0.31 and d_2 = 1.20 to our data. (b) Schematic depicting mixed COOH/OH (upper) and CH_3/OH (lower) monolayers on gold.

the generality of our findings. We use lysozyme as our prototypical protein due to its high structural stability and high net positive charge and study its interaction with mixed monolayers of COOH/OH (Fig. 3). Since the OH component is neutral it does not contribute to the overall surface charge density and therefore the molar fraction of COOH, χ_c, is proportional to the surface charge density. We measured the interaction of lysozyme at 1 μM with 16 surfaces between χ_c = 0–1. Similarly, we measure the interaction of lysozyme with mixed CH_3/OH surfaces. The molar fraction of CH_3, χ_h, is approximately linearly related to the surface contact angle as seen in Fig. 1i and so we use χ_h as a proxy for surface hydrophobicity. The functional form of the coverage *versus* χ_h appears to have a lag phase before rising roughly linearly and then plateauing. The post lag phase rise occurs approximately when the average inter-atom spacing of CH_3 terminating thiols is less than the average dimension of lysozyme (see methods). The coverage of lysozyme on the CH_3/OH surfaces plateaus at roughly half the level seen on the COOH/OH surfaces. We suggest two possible reasons for this. Since charge interactions are described by vector fields, proteins far from the surface can be influenced, leading to multilayer formation. However, the hydrophobic effect is a result of the direct interaction of water molecules with the surface and thus does not influence proteins beyond the interface. It is also possible that if there is a greater affinity of lysozyme to the methyl surface than the carboxyl surface greater structural re-arrangements of lysozyme may occur leading to an increased footprint on the methyl surface. This will allow less lysozyme molecules to cover the surface.

Development of a predictive model

The Langmuir adsorption model was originally designed to describe the interaction of gas molecules at surfaces[7] but more recently has been used to interpret the kinetics of ligand–receptor pair interactions with the QCM.[34] In contrast, the applicability of the Langmuir model to describe protein interactions with solid surfaces is quite controversial[26,35] and yet it is often used due to its simplicity. Furthermore, it is typical to start with the Langmuir equation and then modify it to account for various empirical observations. For the current work we are primarily interested in developing an empirical model that predicts protein adsorption to a reasonable degree of accuracy and are less concerned with whether the Langmuir law or its modified form is a true representation of the interaction dynamics at the molecular level. In the Langmuir model the rate of adsorption of a protein to a surface is given by a first order rate equation where the proteins in solution are assumed to be in dynamic equilibrium with those on the surface:

$$\frac{dm}{dt} = k_a C(m_\infty - m) - k_d m \quad (1)$$

where k_a and k_d are the adsorption and desorption rate constants, with the affinity defined as $K = \frac{k_a}{k_d}$, C is the bulk protein concentration, m is the adsorbed mass at any given time t and m_∞ is the mass of adsorbed protein at maximum coverage. This equation can be solved, leading to an expression that describes how coverage progresses with time:

$$m = \frac{\beta}{\gamma}(1 - e^{-\gamma t}) \quad (2)$$

where $\beta = k_a C m_\infty$ and $\gamma = k_a C + k_d$. We can also relate the equilibrium mass, m_{eq}, to the concentration:

$$m_{eq} = \frac{C m_\infty}{C + K^{-1}} \quad (3)$$

We decided to test the applicability of the Langmuir model to describe the charge driven interactions of lysozyme with mixed COOH/OH surfaces. As χ_c increases so too does the charge density of the surface and we expect the affinity of lysozyme to the surface to increase also. A total of 12 surfaces were chosen with χ_c in the range 0.027–1.0. The coverage of lysozyme on these surfaces was recorded for various concentrations in the range 0.1–20 μM. Based on eqn (2), for one type of protein interacting with a surface (K is constant), we expect as the concentration increases the coverage *versus* time plots will saturate at increasingly large values as shown in the simulation of Fig. 4a. Looking at the raw data (ESI,† Fig. S4) we see good examples of this (χ_c = 0.027 in the range 1–12.5 μM and χ_c = 0.045 in the range 0.1–5.0 μM). In some cases, the concentration and adsorption rate are too low to allow equilibrium to be reached within the timescale of our experiment (for example χ_c = 0.14 in the range 0.01–0.1 μM) and once the surfaces begin to saturate equilibrium coverage is no longer dependent on concentration, as expected. For the Langmuir equation to be valid we would also expect, since $\gamma = k_a C + k_d$, a plot of γ *versus* C to be linear, as previously demonstrated for ligand–pair interactions[34] and yet we observe this only for the very lowest affinity surface χ_c = 0.027 (data not shown). A reason for this could be that the affinity of the proteins to these surfaces is so high that we quickly enter a mass-transport limited situation where the affinity of the protein to the surface is much

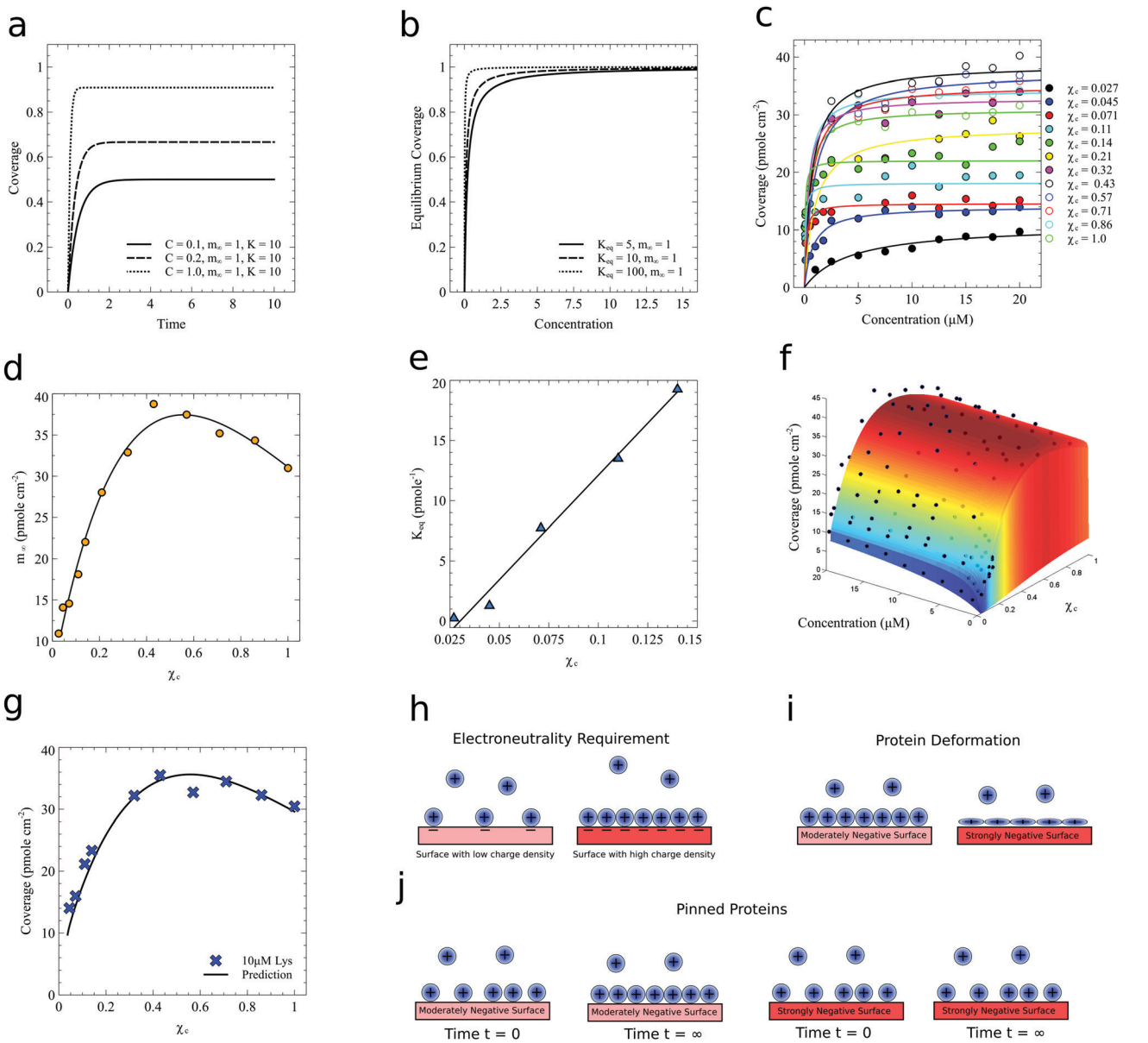

Fig. 4 Adsorption of lysozyme to mixed COOH/OH surfaces and interpretation of molecular-level behaviour through model fitting. (a) The Langmuir kinetic equation, $m = \frac{\beta}{\gamma}(1 - e^{-\gamma t})$ with $\beta = k_a C m_\infty$ and $\gamma = k_a C + k_d$, is used to simulate protein adsorption where concentration varies but protein–surface affinity remains constant. (b) The equilibrium form of the Langmuir equation, $m_{eq} = \frac{C m_\infty}{C + K^{-1}}$, is used to simulate protein adsorption of one protein to different surfaces of varying affinity. (c) Experimental QCM data showing the adsorption of lysozyme in the range 0.01–20 μM to 12 mixed COOH/OH surfaces ranging from χ_c = 0.027–1.0 (circles). Fits to the Langmuir equilibrium equation shown as solid lines. Coverage sampled at t = 400 s, buffer is 10 mM phosphate at pH = 7.4. (d) m_∞ taken from fits in (c) plotted *versus* χ_c and fitted with the empirical model of general form $m_\infty = m_{\infty t}(1 - e^{-\chi_c})e^{-\chi_c}$ (eqn (4)). (e) Equilibrium constant K taken from fits in (c) plotted *versus* χ_c and fitted with a linear relationship. (f) Empirical predictive model (eqn (6)) plotted as heatmap surface together with all 100 experimental data points from (c). Average prediction accuracy 78%. (g) Prediction of coverage (solid line) together with experimental data for lysozyme at 10 μM (blue cross). Average prediction accuracy 93%. (h) Schematic illustrating the requirement of electroneutrality at the solid–liquid interface plane which leads to saturation with concentration at sub-maximal packing. (i) Illustration of sub-maximal packing due to protein deformation at high affinity surfaces leading to increased molecular footprint. (j) Lateral mobility of proteins on low affinity surfaces allows proteins initially adsorbed by a random sequential process to pack maximally over time whereas on high affinity surfaces proteins are 'pinned' which with low lateral mobility leads to sub-maximal packing.

higher than the rate at which protein can be supplied by the pump system. The equilibrium constant for the lowest affinity surface (χ_c = 0.027) was approximately 1 pmole^{-1} or 1×10^{12} M^{-1} which is 4 orders of magnitude larger than that observed by Wu *et al.*[34] for IgG binding to anti-IgG. We also notice that the fits to the rate equation (eqn (2)) are progressively worse for higher χ_c values and increasing concentration. This is a minor effect but likely due to secondary rate effects such as protein re-orientation.

Due to mass transport limitations a more reliable parameter to measure is the equilibrium coverage, m_{eq}. We model the equilibrium coverage as a function of concentration using eqn (3) as shown in Fig. 4b. For one type of protein interacting with surfaces of differing affinity we expect the equilibrium coverage to rise more steeply with concentration as affinity increases. However, the equilibrium coverage should at high concentrations always plateau to the same maximal coverage, m_∞, which should be determined by the point at which the proteins are maximally packed on the surface. Experimental data shown in Fig. 4c demonstrates that m_{eq} does plateau with increased concentration. Remarkably however, in many cases the plateau occurs well below the maximal packing coverage, which is in complete contradiction to the Langmuir equation. As shown in Fig. 4d there is a very clear functional dependence of m_∞ on χ_c. This may be explained by considering the requirement of electroneutrality at the surface. The contribution from proteins to the charge density at the solid–liquid interface plane (in this case a positive charge density) must match the charge density due to the ionized chemical groups of the surface (a negative contribution) as illustrated in Fig. 4h. Considering this effect alone we might expect m_∞ to rise with χ_c approximately linearly at first before saturating as m_∞ approaches the true maximal packing coverage $m_{\infty t}$, which might be described by an equation of general form $m_\infty = m_{\infty t}(1 - e^{-\chi_c})$. However, we see from the data of Fig. 4d that while m_∞ does rise roughly linearly up to $\chi_c = 0.4$, thereafter m_∞ starts to decrease. This effect may be explained by considering that as the affinity of the protein to the surface increases, the large interaction forces experienced may lead to a distortion of the protein structure. This would result in an increased footprint for each protein, thus reducing the number of proteins that can pack onto the surface (Fig. 4i). Another explanation is that even without deformation, as the affinity increases the proteins have less lateral surface mobility. It is known that proteins will typically not adsorb to a surface in the tightest possible hexagonal close packed arrangement but will initially sit on the surface with many gaps too small to pack other proteins in – often referred to as random sequential adsorption.[7,36] It is only through subsequent lateral movement that the proteins reach a tighter packing arrangement. If the lateral movement is limited this process cannot happen, resulting in sub-maximal coverage (Fig. 4j). By applying an exponential decay term, we can approximate the observed behaviour with an equation of the general form $m_\infty = m_{\infty t}(1 - e^{-\chi_c})e^{-\chi_c}$. By including small experimental offsets to m_∞ and χ_c, and with appropriate scaling we devised an empirical model that describes the observed experimental data:

$$m_\infty = (A_1 + B_1[1 - e^{-C_1(\chi_c - D_1)}])e^{-\chi_c/E_1} \quad (4)$$

Fitting to the data we find $A_1 = 10.9$, $B_1 = 213.1$, $C_1 = 0.70$, $D_1 = 0.036$ and $E_1 = 0.73$. From fits of eqn (3) to the data in Fig. 4c we can in principle also extract the affinity constant, K. Correct estimation of K through fitting is crucially dependent on accurate data during the steeply rising portion of the curve at low concentrations. This becomes increasingly difficult to sample as χ_c increases since progressively low concentrations and longer timescales would be required. For 5 surfaces with the lowest χ_c values however we were able to accurately determine the affinity constant as shown in Fig. 4e. We observe a linear relationship between K and χ_c, thus demonstrating that the affinity is strongly related to the surface charge density. The linear fit is given by

$$K = A_2\chi_c + B_2 \quad (5)$$

where $A_2 = 173.4$ and $B_2 = -5.2$. By substituting eqn (4) and (5) into eqn (3) we have an empirical model that describes our data for a range of concentrations and χ_c values:

$$m_{eq} = \frac{C(A_1 + B_1[1 - e^{-C_1(\chi_c - D_1)}])e^{-\chi_c/E_1}}{C + (A_2\chi_c + B_2)^{-1}} \quad (6)$$

This model is plotted in Fig. 4f as a 3D surface, together with all the experimental data. We clearly see the model is a good approximation to the general features of the experimental data. Defining a prediction accuracy as $P = 100\left(1 - \frac{1}{N}\sum_{i=1}^{i=N}\frac{|P_i - m_i|}{m_i}\right)$ where m_i is the experimental data point, P_i is the prediction for that data point and N is the total number of data points, we find $P = 78\%$ for our data. We note for large χ_c values and low concentrations the coverage is overestimated whilst for large χ_c values and high concentrations the model underestimates the coverage. We suspect secondary rate effects, which we have neglected, play a more important role when the coverage is close to the maximal packing coverage at high affinity and concentration. The model is much more accurate at higher concentrations as shown in Fig. 4g for lysozyme at 10 μM, where we observe a prediction accuracy of $P = 93\%$.

Applying the model to real materials

As shown in Fig. 5a we suggest that surfaces can be divided into two broad groups: (a) hydrophilic, charged surfaces; (b) charge neutral surfaces with some degree of hydrophobicity. For example, included in the first group will be charged alkanethiols, metal oxides, charged polymers and charged metals whilst the second group will include hydrophobic alkanethiols, polymers and co-polymers. Protein coverage on materials that are both charged and hydrophobic are likely to be difficult to predict, however most materials relevant to biotechnological and biomedical applications are likely to fall within these two subcategories.

Based on the AFM measurements of the surface potential of OH and COOH terminating alkanethiols and assuming a linear relation between χ_c and the surface potential we find $\psi_s = -21.19\chi_c + 0.646$, where ψ_s is the surface potential in mV. By combining this relation with eqn (6) we can thus predict protein adsorption for lysozyme based only on the concentration and the surface potential. As shown in Fig. 5b we then compared the prediction for hydrophilic charged surfaces to several other protein–surface interactions (Lys-COOH/OH, Cyto-COOH/OH, Lys-Silica, Cyto-Silica), for which we see good agreement. We therefore open the possibility that the model will apply to any material surface for which the surface potential is known or can

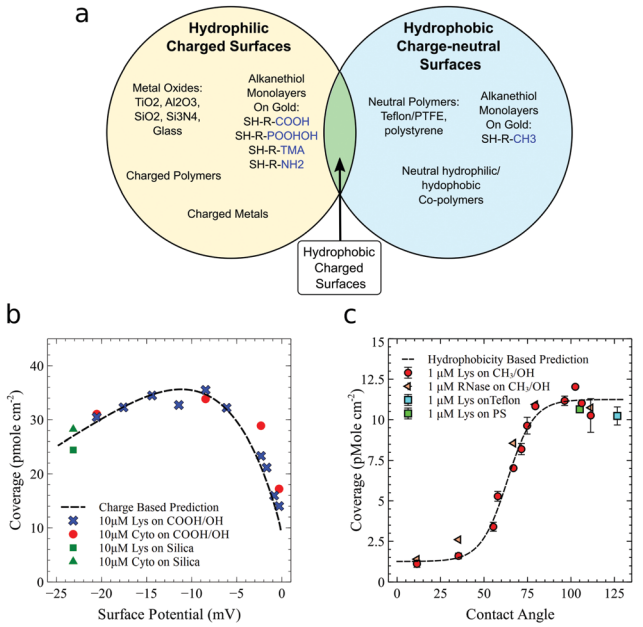

Fig. 5 Predicting protein coverage to real material surfaces. (a) Proposed categorization of material surfaces into two broad groups; hydrophilic charged surfaces and charge-neutral surfaces. (b) Prediction for protein adsorption to charged surfaces with measured potential (dashed line). Tested interactions include lysozyme on COOH/OH mixed monolayers, cytochrome *C* on COOH/OH mixed monolayers, lysozyme on silica and cytochrome *C* on silica (all at 10 μM). (c) Prediction for protein adsorption to neutral surfaces with measured contact angles (dashed line). Tested interactions include lysozyme on CH_3/OH mixed monolayers, ribonuclease-A on CH_3/OH mixed monolayers, lysozyme on PS (polystyrene) and lysozyme on PTFE (polytetrafluoroethylene). Protein concentrations 1 μM.

be measured, and whose surface contact angle is low. Similarly, for the OH/CH_3 surfaces we know from experiment the relation between contact angle and χ_h. For neutral surfaces a coverage prediction can thus be made based on a measurement of the contact angle. For the data where lysozyme interacts with CH_3/OH mixed surfaces we fitted the empirical equation $m = \frac{a_2 10^{b_2(\theta - c_2)}}{1 + 10^{b_2(\theta - c_2)}} + d_2$ with a_2 = 10.0, b_2 = 0.057, c_2 = 63.4, d_2 = 1.25 and θ is the contact angle. As shown in Fig. 5c, we then measured several new protein–surface interactions (Lys – PTFE, Lys – polystyrene, RNase – CH_3/OH) and demonstrate that the measured coverage is in good agreement with the prediction. Whilst these models will need modifications to account for particular structural nuances within the broad spectrum of proteins, we have demonstrated that the two predictive models developed here are broadly applicable to globular proteins interacting with generic materials.

Discussion

Using our survey-style approach where many protein–surface interactions are studied under carefully controlled and homogeneous experimental conditions we are now able to address several key questions that may aid in the rational design of biomaterials and start to settle some of the controversies within the field of protein adsorption:

1. *Do proteins adsorb more to hydrophobic or hydrophilic surfaces?* Under charge-favourable conditions globular proteins adsorb with very high affinity to charged hydrophilic surfaces whilst for unfavourable charge conditions almost no protein adsorbs. Regardless of protein charge state all proteins we studied adsorb to hydrophobic surfaces.

2. *Is charge more important than hydrophobicity?* Both charge and hydrophobicity appear to be equally important for surfaces that are either very hydrophobic or very hydrophilic.

3. *Aren't hydrophilic surfaces resistant to protein adsorption?* Whilst we observe very little adsorption on charge-neutral hydrophilic surfaces, with favourable charge conditions proteins adsorb to a very high extent on hydrophilic surfaces.

4. *Why are PEG and zwitterionic surfaces so good at resisting protein fouling?* It has been argued that steric repulsion and excluded volume effects are responsible for the antifouling properties of PEG.[7,37,38] However, we observe a 95% reduction in protein coverage for charge-neutral hydrophilic (contact angle very low, 11 ± 2°) surfaces. Therefore, whilst steric effects undoubtably play a role, the major reason for surfaces being antifouling is that the two primary drivers of adsorption; charge and hydrophobicity, have been eliminated. Similarly, hydrophilic zwitterionic polymer surfaces[15] typically align their charges in order to present a neutral surface to the protein.

5. *What contact angle constitutes a surface being referred to as hydrophilic?* A consensus on nomenclature is essential when choosing materials for the design of biomaterials as a 'hydrophilic' surface with a contact angle of 65° will behave completely differently to a hydrophilic surface with a contact angle of 10° with regard to protein adsorption. There is no clear definition of what constitutes a hydrophilic surface, however it has been suggested[9] that surfaces with an advancing water contact angle of <65° should be considered hydrophilic (other suggest <90°[39]). This is based on biological responses to surfaces with a spread of ±15°. Interestingly we observe a sigmoidal response of adsorption to surface contact angle with our test protein on mixed OH/CH_3 alkanethiol surfaces. Remarkably the half maximal value was determined to be 63°. However, we observe the onset of the post lag phase rise much earlier, at about 35°. This occurs approximately when the average inter-atom spacing of CH_3 terminating thiols is less than the average dimension of lysozyme. Thus, the requirement is only that hydrogen bonding is disrupted at a length scale comparable to the adsorbing protein and any slight disruption in bonding (manifest by only slight increases in contact angle) can contribute to increased adsorption. Thus hydrophobicity/hydrophilicity as perceived by proteins is not a binary state but a continuum between approximately 35–95°.

6. *Is it appropriate to use the Langmuir equation?* The basic requirements for the Langmuir Law to be a valid approach for describing protein adsorption are:[26] (1) no more than a monomolecular layer should be formed. For most scenarios multilayer formation will occur to some extent but if the rate of multilayer formation is slow compared to the formation of the

first layer and only early timescales are considered the Langmuir equation can be a reasonable approximation; (2) a dynamic equilibrium is maintained. For very high affinity surfaces the off rate will be close to zero and the Langmuir model may appear invalid. Experimental constraints also mean that maintaining enough mass transport is difficult and so as well as equilibrium measurements, the time evolution appears invalid. However, for weakly interacting surfaces we have shown that the coverage plateaus at a value dependent on the solution concentration indicating a dynamic equilibrium is maintained. As shown in Fig. 4e we therefore suspect the equilibrium constants for the 5 weakest surfaces are correct; (3) all adsorption sites are of equal energy. No two surface sites will ever have exactly the same energy, but our surfaces are homogeneous, so this should be good enough; (4) each adsorption site binds an individual protein. For high affinity surfaces proteins will be effectively 'pinned' with very little lateral movement. For weakly interacting surfaces however, lateral movement and high off-rates will permit proteins to rearrange on the surface thus achieving higher packing density than for a typical random sequential adsorption process therefore limiting this effect; (5) the proteins are noninteracting. In the case of lysozyme, we observe a strong dependence of m_∞ on the substrate charge, which should not vary if the classical Langmuir law is valid. We attribute this to the varied effectiveness of the protein charge–charge repulsion and so for charged proteins on weakly interacting charged surfaces the Langmuir law is violated. However, we show that by modifying the Langmuir equation we can develop an empirical model that describes our data with up to 90% accuracy. The final 10% is likely to be due to small contributions from points 1–4. We do not attempt to extract quantitative insights into the kinetics of the adsorption process but instead use this empirical model to aid in predicting extent of adsorption.

7. *Is it possible to predict protein adsorption?* Vogler states that: *''The biophysical chemistry of protein adsorption remains obscure with only a few general ''rules of thumb'' available to guide biomaterials design for specific applications.''* Given that we have a quantitative model that predicts protein adsorption with up to 90% accuracy based only on a measure of the material charge or contact angle we believe our approach to modelling protein adsorption shown in Fig. 5 represents a substantial step forward in this regard. However, clearly there are still many limitations; (a) we studied only small globular proteins and avoided lipidized or glycosylated proteins. It is unclear to what extent large structured proteins such as antibodies and small unstructured peptides will deviate from our model and lipidization/glycosylation has been shown to strongly influence adsorption; (b) solution conditions were of low ionic strength which helps to emphasize the charge dependency of protein adsorption. With increased ionic strength the charge-dependency on adsorption will likely diminish; (c) we only study single component protein solutions which is clearly a much-simplified scenario compared to the myriad of proteins found for example in blood. We hope that this basic research will allow future researchers to gain insights into these more complex systems. However, our model may be more immediately applicable for analytical sensors[40] and protein therapeutics where media is often less complex; (d) the model was developed initially for lysozyme and we show also that other proteins with a high net positive charge behave similarly, but proteins with intermediate net charges will likely deviate. Due to symmetry we expect strongly negatively charged proteins interacting with positively charged surfaces to behave similarly.

Conclusions

By employing a survey-style approach to the study of protein adsorption we have been able address several key questions that have until now remained debatable. We see that net charge and hydrophobicity govern adsorption but to differing extents depending on the relative charge state of protein and surface. Thus, hydrophobic interactions can have both a greater and lesser impact on adsorption compared to charge interactions. We clearly see that just because a surface is hydrophilic does not mean it is protein resistant – with charge favourable conditions proteins adsorb to a very high extent onto hydrophilic surfaces. Conversely, with charge-unfavourable conditions, we see charge-neutral hydrophilic (contact angle around 10°) surfaces present some of the best anti-fouling properties. By employing mixed monolayers with OH/CH_3 chemistry we see that the extent of protein coverage is acutely dependent on surface contact angle and therefore materials should not be classified as either hydrophobic or hydrophilic but considered to sit at a location on a hydrophobicity continuum. We have also shown that while there are many reasons why the Langmuir law may not be applicable to varying extents, the classical Langmuir law completely breaks down for charged proteins interacting with charged surfaces. Through empirical modification of the Langmuir law however we have been able to develop a model that predicts with up to 90% accuracy extent of coverage of proteins to charged surfaces. The two models we have developed for charge-neutral surfaces exhibiting any contact angle (0–125°) and for charged surfaces with low contact angle ($\sim$10°) are broadly applicable, having been tested with various proteins on real materials surfaces including silica, polystyrene and PTFE in addition to the model alkanethiol surfaces. These insights into the general principles that determine protein adsorption to surfaces together with the two quantitative models will allow bioengineers to gauge which materials are most suitable for their application thus allowing the rational design of biomaterials for biomedical and health applications.

Methods

Characterization of surface potential using atomic force microscopy

The interaction force experienced by an AFM cantilever in liquid as it approaches a charged flat substrate is governed by

the Derjaguin, Landau, Verwey and Overbeek (DLVO) theory. This considers the force at any separation to be a sum of the van der Waals interaction and an electrostatic double layer force. In the current work we determine the electrostatic component by numerically solving the full non-linear Poisson–Boltzmann equation, which we demonstrate agrees with previous work[41] as shown in ESI† Fig. S3. We used an Asylum Research MFP3D AFM together with sQube CP-qp-CONT-SiO-C cantilevers (Windsor Scientific Ltd UK) which had a 6.62 μm (±10%) diameter silica microbead attached. The nominal spring constant was 0.1 N m^{-1}. The cantilever holder was cleaned with 2% SDS and water. The open fluid cell and cantilever clip were cleaned by sonication in 2% Hellmanex solution for 5 min followed by washing with copious amounts of water and ethanol. Samples were attached to the bottom of the fluid cell using Dow Corning Vacuum grease. We used 1 mM KCl adjusted to the correct pH with 1 M KOH and 1 M HCl. The lower ionic strength compared to QCM measurements was necessary in order to increase the signal to noise ratio and to match the work of Hillier[41] and meet the requirement of a monovalent salt for the model. Silica samples and cantilevers were cleaned by exposure to oxygen plasma for 10 min. Whilst measurements on silica QCM chips were consistent and reproducible, measurements on alkanethiol coated gold QCM chips were not consistent (in agreement with the work of Hu *et al.*[42]) and so we used ultra-flat template stripped gold (TSG) which was prepared as described previously.[43] Immediately after cleaving the TSG was functionalized in 7 mM alkanethiol solution in ethanol (absolute, Sigma). Approximately 1400 μl of media was used to fill the fluid cell. The cantilever deflection was monitored as the tip was brought towards and away from the surface. Cantilever deflection was converted to a force using an *in situ* measurement of the cantilever resonance peak (thermal spectra) and normal deflection as determined by the contact portion of the force–distance curve. The piezo displacement was converted to a tip-sample separation by subtracting the cantilever deflection. For each sample 100 force–displacement curves were recorded across a 5 μm × 5 μm area. The averaged force–displacement curve was fitted to a numerical solution of the full non-linear Poisson–Boltzmann equation using constant charge boundary conditions as described previously[28,41,42] but implemented using Matlab R2014a (v8.3.0.532). At least 3 separate experiments were conducted for each sample and values averaged.

Static contact angle measurements

Measurements were taken using a goniometer in air (KSV Cam 200, KSV instruments Ltd, Finland). Alkanethiols on gold were incubated for at least 12 hours then washed with absolute ethanol, blown dry with nitrogen gas and immediately measured. A 0.5 μl drop of buffer (10 mM phosphate, pH 7.4), or 1 μl for hydrophobic samples, was formed at the end of the needle. The needle was then lowered until the drop contacted the surface and the needle retracted leaving the droplet on the surface (a larger volume of liquid was needed for very hydrophobic surfaces otherwise the droplet remained on the needle). An optical image was then taken, and the contact angle determined within the software (Attention Theta v4.1.98) using the Young–Laplace algorithm.

QCM preparation

We used a Q-sense E4 QCM from Biolin Scientific (Sweden) and Standard gold coated QCM chips (5 MHz, QCM5140TiAu120-050-Q, Quartz Pro, Sweden). Chips were cleaned using a standard protocol: (a) UV/ozone for 10 minutes; (b) chips placed in a 5 : 1 : 1 mixture of ultrapure water, ammonia (25%) and hydrogen peroxide (30%) at 75 °C for 5 minutes. This solution may cause serious burns, handle with care and take necessary precautions such as using eye protection, gloves and a fume hood; (c) immediate submersion into a beaker of Milli-Q water followed by thorough rinsing under a stream of Milli-Q water; (d) dry with nitrogen gas; (e) UV/ozone treat for 10 minutes. Other chips were purchased from Biolin Scientific including Silicon Dioxide (QSX303) and Teflon AF1600 (QSX 331). Silicon dioxide was cleaned as follows: (a) UV/ozone for 10 minutes; (b) immerse sensors in 2% sodium dodecyl sulfate (SDS) in water for 30 min; (c) rinse with ultrapure water; (d) dry with nitrogen gas; (e) UV/ozone for 10 minutes. Teflon chips were used new from the manufacturer for each experiment and only blown dry with nitrogen gas before use.

QCM chip functionalization

Immediately after cleaning the chips were placed in 200 μl of a 7 mM alkanethiol solution in ethanol (absolute, Sigma). Alkanethiols used were: 11-mercaptoundecanoic acid ($HS(CH_2)_{10}COOH$, Sigma, 674427), 11-mercaptoundecylphosphonic acid ($HS(CH_2)_{11}$-H_2PO_3, Sigma, 754269), 1-undecanethiol ($SH(CH_2)_{10}CH_3$, Sigma, 510467), mercaptoundecyl-hexaethyleneglycol-amine ($SH(CH_2)_{10}$-EG_6-NH_2, Prochimia, TH 002-m11.n6), (11-mercaptoundecyl)-*N*,*N*,*N*-trimethylammonium bromide ($SH(CH_2)_{11}$-*N*-$(CH_3)_3$, Sigma, 733385), 11-mercapto-1-undecanol ($SH(CH_2)_{11}$-OH, Sigma, 674249). Chips remained in the thiol solution for at least 12 hours protected from light. Prior to use the chips were cleaned under a stream of absolute ethanol and dried with nitrogen. The amine terminating thiol also contains ethylene glycol (EG) repeats as we found this was required for the amine to be protonated at neutral pH. Previously[44,45] it has been shown that whilst primary amines in bulk are protonated at neutral pH[46] (pK = 10.6), the pK of surface confined amines is much lower (pK ≈ 4) and therefore unprotonated and neutral. This is attributed to the disordered structure of the SAM in this case which creates a hydrophobic environment. By using SH-$(CH_2)_{10}$-EG_6NH_2 we were able to create a hydrophilic environment for the primary amine.

QCM experiment

The frequency change of the resonator is related to the adsorbed areal mass density by the Sauerbrey equation,[30,47] which in turn we convert to an areal molar density, which is a more useful parameter when comparing different proteins.

Since the surface bound nanoscale globular proteins represent a laterally heterogenous film the Sauerbrey equation is only valid[30] if $\Delta D/(\Delta f/n) \ll 4 \times 10^{-7}$. As shown in ESI† Table S2 this is true for all the proteins presented here. We also tabulate the raw data in ESI† Tables S3–S5. Alkanethiol functionalized chips were allowed to equilibrate in buffer (10 mM phosphate, pH 7.4) for a few hours in order to obtain a stable baseline. Buffers were degassed prior to use. The same buffer used to obtain the baseline was always then used to prepare the protein solutions. Proteins used were: ribonuclease A from bovine pancreas (RNase, Sigma, R6513), myoglobin from equine skeletal muscle (Myo, Sigma, M0630), bovine apo-transferrin (Trans, Sigma, T1428), alpha-lactalbumin from bovine milk (α-Lact, Sigma, L5385), lysozyme from chicken egg white (Lys, Sigma, L6876), bovine serum albumin (BSA, Sigma, 05470), alpha-chymotrypsinogen A from bovine pancreas (Chymo, Sigma, C4879), cytochrome *C* from equine heart (Cyto, Sigma, C2506), beta-lactoglobulin A from bovine milk (β-Lact, Sigma, L7880), albumin from chicken egg white (Oval, Sigma, A5503-1G). All protein solutions were prepared fresh before each experiment. A volume of 1.8 ml of protein solution was flowed into the QCM chamber at a rate of 100 μl min^{-1} and the frequency shift monitored in real time after which time flow was stopped and protein exchanged for buffer, which was flowed for a further 1.6 ml. Protein concentrations for Fig. 2 and 3 were 1 μM and in the range 0.01–20 μM for Fig. 4. The chamber temperature was maintained at 25 °C.

QCM data analysis

All data was analysed using custom routines developed in Matlab R2014a. Raw data was collected using QSoft401 (v2.5.22.707) and was converted to .txt files to be read by matlab using QTools (v3.1.27.609). Frequency shifts of the $n = 5$ harmonic were converted to mass using the Saurbrey equation. Where specified areal mass was sampled at $t = 400$ s from the onset of the frequency shift. Areal mass was then converted to coverage (areal mole density) by dividing by molecular weight.

Calculation of inter-atom spacing of CH_3/OH alkanethiols

Assuming a random distribution of CH_3 groups across the surface we would expect a mean separation distance of CH_3 groups, d, to be approximately $d = \frac{a}{f_0}$ where f_0 is the fractional occupancy of available sites and a is the minimal adatom separation. Assuming[48] $(\sqrt{3} \times \sqrt{3})R30^\circ$ registry with the Au(111) and a Au nearest neighbour separation of 0.29 nm we can assume the nearest neighbour separation of alkanethiols is $a \approx 0.5$ nm. With $f_0 \approx \chi_h$ we have $d\,[\mathrm{nm}] = 0.5/\chi_h$. Given that the end of the lag phase occurs at approximately $\chi = 0.2$ we find $d \approx 3$ nm, which is comparable to the dimension of lysozyme.[49]

DPI experiments

We used an Analight 4D dual polarization interferometer (Farfield-Biolin Scientific AB, Sweden). Chips were cleaned as follows: (a) UV/ozone for 10 minutes; (b) wash ultrapure water; (c) place in 2% sodium dodecyl sulfate (SDS) for 20 min; (d) rinse with ultrapure water and ethanol and dry in a stream of dry nitrogen. The experimental setup has been described in more detail previously.[50] Protein solutions of 1 μM were flowed across the chips at a rate of 50 μl min^{-1} for 200 μl and the dry mass sampled at 2 min.

Conflicts of interest

There are no conflicts to declare.

Acknowledgements

This work was supported by MedImmune Ltd.

References

1 J. M. Anderson, A. Rodriguez and D. T. Chang, Foreign body reaction to biomaterials, *Semin. Immunol.*, 2008, **20**, 86–100.
2 J. D. Andrade and V. Hlady, Protein Adsorption and Materials Biocompatibility: A Tutorial Review and Suggested Hypothesee, *Adv. Polym. Sci.*, 1986, **79**, 1–63.
3 D. Costa, P. A. Garrain and M. Baaden, Understanding small biomolecule-biomaterial interactions: a review of fundamental theoretical and experimental approaches for biomolecule interactions with inorganic surfaces, *J. Biomed. Mater. Res., Part A*, 2013, **101**, 1210–1222.
4 J. D. Andrade, V. Hlady and A. P. Wei, Adsorption of complex proteins at interfaces, *Pure Appl. Chem.*, 1992, **64**, 1777–1781.
5 K. Nakanishi, T. Sakiyama and K. Imamura, On the Adsorption of Proteins on Solid Surfaces, a Common but Very Complicated Phenomenon, *J. Biosci. Bioeng.*, 2001, **91**, 233–244.
6 J. J. Gray, The interaction of proteins with solid surfaces, *Curr. Opin. Struct. Biol.*, 2004, **14**, 110–115.
7 M. Rabe, D. Verdes and S. Seeger, Understanding protein adsorption phenomena at solid surfaces, *Adv. Colloid Interface Sci.*, 2011, **162**, 87–106.
8 C. Pinholt, R. A. Hartvig, N. J. Medlicott and L. Jorgensen, The importance of interfaces in protein drug delivery – why is protein adsorption of interest in pharmaceutical formulations?, *Expert Opin. Drug Delivery*, 2011, **8**, 949–964.
9 E. A. Vogler, Protein adsorption in three dimensions, *Biomaterials*, 2012, **33**, 1201–1237.
10 W. Norde, My voyage of discovery to proteins in flatland . . .and beyond, *Colloids Surf., B*, 2008, **61**, 1–9.
11 M. Ozboyaci, D. B. Kokh, S. Corni and R. C. Wade, Modeling and simulation of protein–surface interactions: achievements and challenges, *Q. Rev. Biophys.*, 2016, **49**, 1–45.
12 Z. Adamczyk, Modeling adsorption of colloids and proteins, *Curr. Opin. Colloid Interface Sci.*, 2012, **17**, 173–186.

13 K. Nakanishi, T. Sakiyama and K. Imamura, On the adsorption of proteins on solid surfaces, a common but very complicated phenomenon, *Biosci. Bioeng.*, 2001, **91**, 233–244.
14 P. Parhi, A. Golas and E. A. Vogler, Role of proteins and water in the initial attachment of mammalian cells to biomedical surfaces: a review, *J. Adhes. Sci. Technol.*, 2010, **24**, 853–888.
15 L. Shen and J. Zhu, Heterogeneous surfaces to repel proteins, *Adv. Colloid Interface Sci.*, 2016, **228**, 40–54.
16 M. Rodahl, F. Hook, A. Krozer, P. Brzezinski and B. Kasemo, Quartz-Crystal Microbalance Setup for Frequency and Q-Factor Measurements in Gaseous and Liquid Environments, *Rev. Sci. Instrum.*, 1995, **66**, 3924–3930.
17 I. Carton, A. R. Brisson and R. P. Richter, Label-free detection of clustering of membrane-bound proteins, *Anal. Chem.*, 2010, **82**, 9275–9281.
18 K. Prime and G. Whitesides, Self-assembled organic monolayers: model systems for studying adsorption of proteins at surfaces, *Science*, 1991, **252**, 1164–1167.
19 E. Ostuni, L. Yan and G. M. Whitesides, The interaction of proteins and cells with self-assembled monolayers of alkanethiolates on gold and silver, *Colloids Surf., B*, 1999, **15**, 3–30.
20 P. Roach, D. Farrar and C. C. Perry, Interpretation of protein adsorption: surface-induced conformational changes, *J. Am. Chem. Soc.*, 2005, **127**, 8168–8173.
21 H. T. M. Phan, S. Bartelt-Hunt, K. B. Rodenhausen, M. Schubert and J. C. Bartz, Investigation of bovine serum albumin (BSA) attachment onto self-assembled monolayers (SAMs) using combinatorial quartz crystal microbalance with dissipation (QCM-D) and spectroscopic ellipsometry (SE), *PLoS One*, 2015, **10**, e0141282.
22 A. Sethuraman, M. Han, R. S. Kane and G. Belfort, Effect of surface wettability on the adhesion of proteins, *Langmuir*, 2004, **20**, 7779–7788, DOI: 10.1021/la049454q.
23 E. Ostuni, B. A. Grzybowski, M. Mrksich, C. S. Roberts and G. M. Whitesides, Adsorption of proteins to hydrophobic sites on mixed self-assembled monolayers, *Langmuir*, 2003, **19**, 1861–1872, DOI: 10.1021/la020649c.
24 E. Ostuni, R. G. Chapman, R. E. Holmlin, S. Takayama and G. M. Whitesides, A survey of structure-property relationships of surfaces that resist the adsorption of protein, *Langmuir*, 2001, **17**, 5605–5620, DOI: 10.1021/la010384m.
25 E. Ostuni, R. G. Chapman, M. N. Liang, G. Meluleni, G. Pier, D. E. Ingber and G. M. Whitesides, Self-Assembled Monolayers That Resist the Adsorption of Cells, *Langmuir*, 2001, **17**, 6336–6343, DOI: 10.1021/la010552a.
26 R. A. Latour, The Langmuir isotherm: A commonly applied but misleading approach for the analysis of protein adsorption behavior, *J. Biomed. Mater. Res., Part A*, 2015, **103**, 949–958.
27 W. A. Ducker, T. J. Senden and R. M. Pashley, Direct measurement of colloid forces using atomic force microscope, *Nature*, 1991, **353**, 239–241.
28 H.-J. Butt, K. Graf and M. Kappl, *Physics and chemistry of interfaces*, Wiley-VCH, 2013.
29 C. D. Bain, E. B. Troughton, Y. T. Tao, J. Evall, G. M. Whitesides and R. G. Nuzzo, Formation of Monolayer Films By the Spontaneous Assembly of Organic Thiols From Solution Onto Gold, *J. Am. Chem. Soc.*, 1989, **111**, 321–335.
30 I. Reviakine, D. Johannsmann and R. P. Richter, Hearing What You Cannot See and Visualizing What You Hear, *Anal. Chem.*, 2011, **83**, 8838–8848.
31 G. H. Cross, Y. Ren and N. J. Freeman, Young's fringes from vertically integrated slab waveguides: applications to humidity sensing, *J. Appl. Phys.*, 1999, **86**, 6483.
32 J. Escorihuela, M. Á. González-Martínez, J. L. López-Paz, R. Puchades, Á. Maquieira and D. Gimenez-Romero, Dual-polarization interferometry: a novel technique to light up the nanomolecular world, *Chem. Rev.*, 2015, **115**, 265–294.
33 K. L. Prime and G. M. Whitesides, Adsorption of Proteins Onto Surfaces Containing End-Attached Oligo(Ethylene Oxide) – a Model System Using Self-Assembled Monolayers, *J. Am. Chem. Soc.*, 1993, **115**, 10714–10721.
34 Y. Wu, H. Ma, D. Gu and J. He, A quartz crystal microbalance as a tool for biomolecular interaction studies, *RSC Adv.*, 2015, **5**, 64520–64525.
35 J. J. Ramsden, Puzzles and paradoxes in protein adsorption, *Chem. Soc. Rev.*, 1995, **24**, 73.
36 P. Schaaf and J. Talbot, Surface exclusion effects in adsorption processes, *J. Chem. Phys.*, 1989, **91**, 4401–4409.
37 S. I. Jeon, J. H. Lee, J. D. Andrade and P. G. De Gennes, Protein-surface interactions in the presence of polyethylene oxide. I. Simplified theory, *J. Colloid Interface Sci.*, 1991, **142**, 149–158.
38 M. Morra, On the molecular basis of fouling resistance, *J. Biomater. Sci., Polym. Ed.*, 2000, **11**, 547–569.
39 R. Forch, H. Schonherr, A. Tobias and A. Jenkins, *Surface design: applications in bioscience and nanotechnology*, 2009.
40 S. A. Bhakta, E. Evans, T. E. Benavidez and C. D. Garcia, Protein adsorption onto nanomaterials for the development of biosensors and analytical devices: a review, *Anal. Chim. Acta*, 2015, **872**, 7–25.
41 A. C. Hillier, S. Kim, A. J. Bard, A. C. Hillier, S. Kim and A. J. Bard, Measurement of Double-Layer Forces at the Electrode/Electrolyte Interface Using the Atomic Force Microscope: Potential and Anion Dependent Interactions, *J. Phys. Chem.*, 1996, **3654**, 18808–18817.
42 K. Hu and A. J. Bard, Use of Atomic Force Microscopy for the Study of Surface Acid−Base Properties of Carboxylic Acid-Terminated Self-Assembled Monolayers, *Langmuir*, 1997, **13**, 5114–5119.
43 S. J. Attwood, A. M. C. Simpson, R. Stone, S. W. Hamaia, D. Roy, R. W. Farndale, M. Ouberai and M. E. Welland, A simple bioconjugate attachment protocol for use in single molecule force spectroscopy experiments based on mixed self-assembled monolayers, *Int. J. Mol. Sci.*, 2012, **13**, 13521–13541.

44 D. V. Vezenov, A. Noy, L. F. Rozsnyai and C. M. Lieber, Force Titrations and Ionization State Sensitive Imaging of Functional Groups in Aqueous Solutions by Chemical Force Microscopy Force Titrations and Ionization State Sensitive Imaging of Functional Groups in Aqueous Solutions by Chemical Force Microscopy, *J. Am. Chem. Soc.*, 1997, **119**, 2006–2015.

45 W. A. Marmisolle, D. A. Capdevila, E. De Llave, F. J. Williams and D. H. Murgida, Self-Assembled Monolayers of NH_2 – Terminated Thiolates: Order, pKa, and Specific Adsorption, *Langmuir*, 2013, **29**, 351–359.

46 D. R. Lide, *Handbook of Chemistry and Physics*, CRC Press, 84th edn, 2003.

47 G. Sauerbrey, Verwendung von Schwingquarzen zur Wägung dünner Schichten und zur Mikrowägung, *Z. Phys. Chem.*, 1959, **155**, 206–222.

48 R. Colorado Jr and T. R. Lee, Thiol-based Self-assembled Monolayers: Formation and Organization, *Encycl. Mater. Sci. Technol.*, 2001, 9332–9344.

49 T. Arai and W. Norde, The behavior of some model proteins at solid-liquid interfaces 1. Adsorption from single protein solutions, *Colloids Surf.*, 1990, **51**, 1–15.

50 K. Xu, M. M. Ouberai and M. E. Welland, A comprehensive study of lysozyme adsorption using dual polarization interferometry and quartz crystal microbalance with dissipation, *Biomaterials*, 2013, **34**, 1461–1470.